Motion of contrast envelopes: peace and noise

Simon J. Cropper

Department of Physiology, University of Melbourne (non-private), Victoria 3010, Australia

Alan Johnston

Department of Psychology, University College London, Gower Street, London WC1E 6BT, UK

Received November 29, 2000; revised manuscript received May 3, 2001; accepted June 5, 2001

We examined the effect of changing the composition of the carrier on the perception of motion in a drifting contrast envelope. Human observers were required to discriminate the direction of motion of contrast modulations of an underlying carrier as a function of temporal frequency and scaled (carrier) contrast. The carriers were modulations of both color and luminance, defined within a cardinal color space. Random-noise carriers had either binary luminance profiles or flat (gray-scale–white) or $1/f$ (pink) spectral power functions. Independent variables investigated were the envelope spatial frequency and temporal-drift frequency and the fundamental spatial frequency, color, and temporal-update frequency of the carrier. The results show that observers were able to discriminate correctly the direction of envelope motion for binary-noise carriers at both high (16 Hz) and low (2 Hz) temporal-drift frequencies. Changing the carrier format from binary noise to a flat (gray-scale) or $1/f$ amplitude profile reduced discrimination performance slightly but only in the high-temporal-frequency condition. Manipulation of the fundamental frequency of the carrier elicited no change in performance at the low temporal frequencies but produced ambiguous or reversed motion at the higher temporal frequencies as soon as the fundamental frequency was higher than the envelope modulation frequency. We found that envelope motion detection was sensitive to the structure of the carrier.

OCIS codes: 330.4150, 330.5510, 330.0330, 330.6790.

1. INTRODUCTION

Previous work concerning our ability to discriminate the direction of motion of contrast modulation has concentrated on the effect that varying the envelope structure has upon performance. This emphasis has tended to lead to the assumption that the structure of the carrier is relatively unimportant as a determinant of psychophysical performance. In the current paper we examine this assumption. In particular, we show that the spectral composition of the carrier is critical in determining the response of the observer.

The supposition that the exact form of the carrier has little effect on envelope encoding can be traced to the prevailing view that the envelope and the carrier form separate parts of the input that are processed essentially independently. In this view an initial spatiotemporal filtering stage is followed by some appropriate nonlinear operation such as squaring or rectification. This hierarchical arrangement allows the generation of a pseudo-first-order signal, a distortion product[1] within the neural representation of the image. This signal is then assumed to be detected in the same way as a real signal, i.e., one that is present in the input image. Given that the envelope will modulate all carrier spatial frequencies equally, the expectation is that the precise form of the carrier will not influence the fundamental aspects of the distortion product such as its temporal or spatial frequency. Recent work, however, has shown that the carrier format and content is a critical factor in the discrimination of the direction of motion of a contrast envelope.[2–6]

Originally studies on the motion of contrast envelopes used either amplitude modulated gratings or beats, a particular kind of amplitude modulated grating.[7–12] Later work adopted random-dot noise fields as carriers, but important differences between two-dimensional multiple-scale carriers on the one hand and single grating carriers on the other[13–20] and their consequences for perception were not examined.

Generally, work using single-scale grating carriers led to the conclusion that the detection and discrimination of motion in contrast-modulated patterns was not mediated by a distortion product resulting from a nonlinear stage before spatial filtering.[21,22] It was shown that observers' abilities to discriminate motion in contrast-modulated patterns were very different from their abilities to discriminate motion in luminance modulated patterns of the same modulation frequency[9–11,23] and there seemed to be little interaction between luminance and contrast modulations. These results were most consistent with an explicit contrast-gradient sensitivity rather than with envelope extraction by a squaring or rectification operation.[9,11,24] Indeed, these differences in the data for contrast- and luminance-based motion were such that it seemed unlikely that even an arbitrary late nonlinearity (i.e., after spatial filtering) underlies performance. Subsequent research using two-dimensional random-noise fields, however, led to the suggestion that tends to predominate in the literature, that a separate nonlinear pathway is responsible for the detection of motion in contrast-modulated patterns. The proposal generated from the data (largely using broadband carriers) is that the nonlinearity is of the form of a squaring or full-wave

rectification and that it occurs after initial spatial filtering but before motion extraction, which is performed by a similar method for both luminance- and contrast-based motion.[13–20]

Later work using the two major types of carrier (gratings and two-dimensional binary noise) provides further evidence of carrier dependence. For example, the perceived speed of an envelope with a static sinusoidal carrier was found to be underestimated,[25] whereas the perceived speed of an envelope modulating two-dimensional binary noise carriers was approximately veridical.[19,26] It is also the case that the perceived direction of motion of a plaid pattern constructed from second-order components is critically dependent on the orientation content of the carrier.[2,27,28] It is this kind of relatively subtle difference in performance that has characterized much of the data and has made the job of discriminating among particular theories about the specific nature of the underlying mechanisms difficult.

The experiments described below address the difference in performance between single- and multiple-scale carriers by gradually changing the carrier composition. To this end we use carriers ranging between a single grating and a multiple-component noise carrier and examine performance in a direction-discrimination task as a function of carrier contrast, temporal frequency, and spatial frequency profile.

2. METHODS

A. Apparatus and Stimuli

All patterns were digitally generated from sinusoidal modulations of color or luminance and were displayed to a contrast resolution of 14 bits by a VSG2/3 (Cambridge Research Systems) stimulus generator. The patterns were presented on a Sony SEII color monitor with a mean luminance and chromaticity of 90 cd/m^2, CIE coordinates (x:0.333 y:0.377). The monitors were driven at a frame rate of 75 Hz and a line rate of 52 kHz, with all patterns combined digitally before presentation. The voltage-to-luminance relationship of the display was measured with a photometric head (Graseby S351G), and the nonlinear relationship was corrected using internal lookup tables on the VSG. The curve-fitting procedure gave an R value accounting for 0.998 of the variance. The display subtended a visual angle of 30° by 24° at the viewing distance of 0.5 m. The sensitivity of the observer to the carrier for each pattern was measured independently under each set of conditions. A small dark fixation point was located at the center of the display. Viewing was conducted in a semidarkened room and was binocular with natural pupils. No head restraint was used. Observers were one of the authors (SJC) and four paid observers naïve as to the aim of the experiment (MW, RM, RB, and SB).

The stimuli were one dimensional and horizontal. Their chromatic properties are described by a vector in a cardinal color space characterized by using the coordinate system of Derrington *et al.*[29] The subjective equiluminant point for each of the chromatic stimuli was found by using heterochromatic flicker photometry performed under conditions as close as possible to the subsequently presented chromatic test stimulus.[30,31] All stimuli were presented in a centrally located 20° disk within a raised-cosine temporal envelope of 500-ms half-width.

B. Construction of the Stimuli

The stimuli presented in this paper are sinusoidal modulations in the contrast of a carrier. The carriers consist of a first-order modulation in the spatial luminance or chromatic profile and either were a single grating component, and therefore contained luminance modulation at a single spatial scale, or were made from multiple grating components and consequently contain multiple spatial scales. The one-dimensional noise carriers were constructed in two different ways. Equivalence between the methods can be verified mathematically. As a *post hoc* analysis, the stimulus profiles calculated were selected at random and were analyzed for their components to ensure that the stimuli were exactly as reported. This condition is critical to the argument presented in the paper.

The default method for constructing noise carriers, i.e., that which has been used by most previous authors, is to use a pseudo-random-noise-generation algorithm (in this case random-number-generation algorithm Ran4( )[32]) and create the desired spatial data directly from the output of this algorithm. The brightness of the individual pixels (or lines) is then either restricted to binary values or left as a gray-scale profile. This method was used principally to calculate the one-dimensional binary noise used in the current experiments.

An alternative and more convenient method, given the aims of the current paper, was to construct the first-order carrier by directly adding sinusoids of given frequency and phase. This Fourier synthesis technique makes controlling the fundamental frequency and spectral composition of the noise straightforward and reliable. The one-dimensional gray-scale and 1/f noise carriers were made with this method.

Psychophysical performance in a direction-discrimination task for these multiple-scale carriers was compared with performance with single-scale grating carriers: an amplitude-modulated grating.[24,33,34] A general description of an amplitude-modulated grating is shown in Eq. (1):

$$L(y,t) = L_m\{1 + C_c \sin 2\pi(f_c y + \phi_c) \times 0.5[1 + M \cos 2\pi(f_{\mathrm{env}} y + w_{\mathrm{env}} t + \phi_{\mathrm{env}})]\}, \quad (1)$$

where M is the depth of modulation ($0 \leq M \leq 1$) of carrier contrast (C_c), f_c is the spatial frequency of carrier in cycles per degree (cpd) and f_{env} is the spatial frequency of the contrast envelope. Spatial phase angle of carrier and envelope are denoted by ϕ_c and ϕ_{env}, respectively. Since the only movement in the carrier in the work described here is a random updating of its spatial phase (ϕ_c; see below), only the envelope has a temporal frequency term w_{env}(Hz). It should be clear that Eq. (1) describes a carrier grating modulated by a raised-cosine spatial-contrast envelope; the mean carrier contrast remains constant whatever the modulation depth M.

In the case of the noise carriers a more general equation may be given (Rand_wave may also be the single grating above):

$$L(y,t) = L_m\{1 + C_c[\text{Rand\_wave}(f_c y + \phi_1)] \times 0.5[1 + M\cos 2\pi(f_{\text{env}} y + w_{\text{env}} t)]\}, \quad (2)$$

where again M is the depth of modulation (0–1) of carrier contrast C_c and f_c is the carrier fundamental frequency (0.125 cpd for the binary noise, as described for flat gray scale and $1/f$ noise) and Rand_wave is the carrier-noise waveform (amplitude range ±1.0). The majority of the stimuli, indeed all unless otherwise noted, have 100% modulated contrast envelopes, $M = 1$.

C. Manipulation of the Fundamental Frequency

A major feature of this study is the control of the fundamental frequency of the spatial profile of a noise carrier. The motivation for this manipulation comes from considering the change in carrier composition that occurs in moving from a single grating to a composite noise pattern and what this entails. It would be unusual to use a contrast-modulated grating in which the carrier grating was at a lower spatial frequency than the contrast envelope. Intuitively, one would imagine such a grating to contain a luminance modulation moving with the envelope.

Many studies use noise carriers where the noise has been produced by some random-number-generation algorithm and then subjected to multiplication by a contrast envelope. These stimuli are drift balanced in that their expected power spectra are symmetrical with respect to the spatial frequency axis.[13] It is important to note that the expected power is symmetric only because it is uniform. For any instantiation of a drift-balanced stimulus this symmetrical relationship does not hold, because the power spectrum of a given sample of noise is structured. For contrast-modulated noise the power spectrum in the upper quadrants is shifted along the spatial frequency axis relative to the identical power spectrum in the lower quadrant, which shifts in the opposite direction by an equal amount that depends on the envelope's spatial frequency [see Fig. 1(c)]. Typically, the modulation direction and speed of motion are clearly visible in the spectrum as local oriented energy.[35] When the carrier is dynamic the same is true for each temporal frequency component in the noise. This can lead to a bias in the spatiotemporal frequency content that differs for each instantiation. If for each instantiation of a drift-balanced stimulus the power spectrum was flat and unbounded, then limiting factors such as the spatial and temporal resolution of visual processing should have no effect on the relative power in opposite quadrants of the power spectrum of the transformed stimulus. Since for any given stimulus the power spectrum is structured, the limits of visibility can determine perceived direction of motion. The visual system may exploit this bias on an instant-by-instant basis. The experiments described below are designed to investigate whether this is the case.

To take an alternative approach, if one examines these stimuli in terms of their sinusoidal components and takes each component independently for a given contrast envelope, an equation can be generated that describes the stimulus characteristics at each scale. This is a similar but slightly different way of representing the stimulus but is most suited to the current argument.

At a given scale and in one spatial dimension, a grating component of the contrast-modulated noise stimulus (100% modulated envelope) can be represented as

$$L(y,t) = (\cos A + 1)\cos B, \quad (3)$$

where $A = ay + wt$ and represents the envelope, and $B = by$ and represents the grating component of the carrier in question.

Equation (3) can be expanded to

$$L(y,t) = \cos A \cos B + \cos B. \quad (4)$$

With use of the identity

$$\cos A \cos B = 1/2[\cos(A + B) + \cos(A - B)],$$

Eq. (4) becomes

$$L(x,t) = 1/2[\cos(ay + wt + by) + \cos(ay + wt - by)] + \cos(by), \quad (5)$$

which simplifies to

$$L(x,t) = 1/2\{\cos[(a + b)y + wt] + \cos[(a - b)y + wt]\} + \cos(by). \quad (6)$$

$\text{Cos}(by)$ describes the static carrier grating; the other terms relate to the envelope. The symbols a and b represent the spatial frequency of the envelope and of the carrier, respectively [Fig. 1(a)]. Note that if $a < b$, $a > 0$, and $b > 0$ (i.e., the carrier is a higher spatial fre-

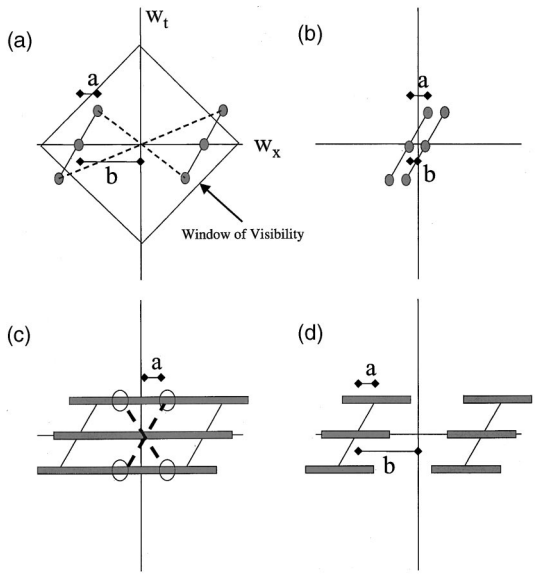

Fig. 1. Schematic Fourier transforms: (a) The amplitude spectrum of an amplitude modulated grating with carrier spatial frequency b and envelope spatial frequency a. (b) When the spatial frequency of the carrier is less than the spatial frequency of the envelope, all components fall in the quadrants corresponding to motion in the same direction as that of the envelope. (c) Modulation of broadband noise results in an approximately flat spectrum, although there will be different variations in level for each instantiation of noise (not shown). Each component is shifted as in (a) and (b). (d) A lower bound can be placed on noise carriers such that for all components the relationship seen in (b) is avoided.

quency than the envelope as is normally the case for single-scale carriers), then $a + b > 0$ and $a - b < 0$.

The signature of rigid motion in the Fourier transform of a space–time representation of the moving stimulus is that the energy is limited to a line through the frequency-space origin. Energy distributed within the upper-right and lower-left quadrants indicates motion in one direction, and energy in the other diagonally opposite quadrants indicates motion in the opposite direction. The movement of contrast modulations can be said to produce off-axis-oriented structure in the Fourier transform [Figs. 1(a)–1(d)] in that the additional components introduce oriented energy but the distribution does not fall on a line through the origin. This is simply a description of the appearance of the Fourier transform of the stimulus.[1,35,36]

The transform can be thought of as the modulation of a carrier in the case in which the components on the left and right of Fig. 1(a) are grouped. The slope of these local Fourier energies depends on envelope velocity, and their position on the spatial frequency axis depends on the carrier spatial frequency. Alternatively, the three pairs of components connected through the origin can be grouped. In this organization the transform is considered to be the sum of two gratings moving in opposite directions and one static grating. Either interpretation is equally valid. When the carrier spatial frequency is lower than the envelope spatial frequency, as in Fig. 1(b), one component in the additive combination interpretation switches direction, and now all moving components are in the envelope direction. Note that if the high-spatial-frequency component is removed by filtering or by the limited resolution of the visual system, only the additive interpretation is valid, and the transform then represents the addition of one moving and one static grating.

The situation in which the envelope is at a higher spatial frequency than the carrier ($a > b$) will occur in a random-noise stimulus if the lowest spatial frequency present in the noise is not controlled such that it is always higher than the envelope spatial frequency. This situation is depicted in Fig. 1(c). The lowest spatial frequency present in unfiltered noise is one cycle per image. There will also be variation in the nonzero mean level: a dc component. Unless the carrier is explicitly filtered or controlled in some other way, contrast-modulated random noise will contain oriented Fourier energy, which passes through the origin at (due to the modulation of the dc component), or close to, the envelope temporal frequency [Fig. 1(c)]. This Fourier component could mediate direction discrimination. What actually happens depends on how all the (sideband) components are combined in the composite image [Fig. 1(c)]. Modulation will also generate energy for the opposite direction, but the energy will not necessarily be the same in each quadrant in this case [see Fig. 1(c)].

In studying the detection of motion of contrast envelopes, we would ideally wish to avoid modulation of components that introduce energy into adjacent quadrants of the frequency space, as this would be equivalent to adding a rigid motion in the envelope direction to the stimulus. By placing a lower bound on the carrier power spectrum, we can ensure that drifting contrast modulation does not introduce energy in other quadrants in frequency space [Fig. 1(d)]. This process essentially etches the spatiotemporal power spectrum, removing energy differentially from the two sets of diagonal quadrants. Note that in the case of an amplitude-modulated grating, if the carrier spatial frequency is less than the envelope spatial frequency ($a > b$), filtering out the high-spatial-frequency component should not lead to the perception of motion in a direction opposite to the envelope motion [see Fig. 1(b)]. Therefore, unless there is a lower bound on a broadband carrier, one would not predict reversal of motion in the case of broadband carriers, although one may see the reversal of motion for narrow-band carriers for the same envelope motion. This carrier-dependent behavior may be misinterpreted as evidence for multiple mechanisms or simply be attributed to a discrepancy in the data on envelope motion perception. In comparing data for different carriers it is important to be sensitive to this kind of manipulation.

Another issue worthy of comment is the effect of making the noise carrier dynamic. This process is examined experimentally below, but the manipulation is introduced at this stage. It has been stated that such a manipulation removes any artifact.[2,3,5,6] Updating the carrier as the envelope drifts over it introduces energy throughout the spatiotemporal spectrum. Modulation by a sine wave in the spatiotemporal domain is equivalent to convolving this spatiotemporal spectrum with the transform of the sine wave in the Fourier domain,[36] in effect placing multiple copies of the envelope spectrum at each point in the noise spectrum. This can balance the spectrum for leftward and rightward motion if the envelope and carrier have the same update rate. The dynamic carriers in this paper and, it is worthwhile noting, many previous publications, are updated at 25 Hz, while the envelope may be updated at each frame (75 Hz) depending on the drift frequency. This point will be raised again in Fig. 15 below, where we will show that the critical aspects of our data, most notably the carrier dependence of the perception of forward motion in rapidly drifting envelopes, remain even when the stimulus is microbalanced and drift balanced (75-Hz carrier and envelope update), and the window of visibility should not be able to explain our data.[6] At this stage in the paper, the point is that a lower bound has to be placed on the spatial frequency content of the noise if one wishes to compare the effects of modulations on dynamic carriers, static carriers, and gratings, without having to consider the effects of adding new components that move in the envelope direction or the relationship between the carrier and envelope update rates.[2,3,5,6]

Empirically, there are two critical issues with respect to the current experiments. The first question is whether removing the lowest spatial frequencies in the carrier still allows accurate direction discrimination at high temporal drift frequencies. This is important because it is at high temporal frequencies that one sees clear differences between the data for single- and multiple-scale carriers. The second and related issue is whether removing low spatial frequencies in the carrier can generate direction reversals in static and dynamic noise carriers. As discussed above, these stimuli have a more complex component structure than amplitude-modulated gratings and beats, both of which have been shown to generate strong

reversals in perceived direction at high temporal drift frequencies, an effect most easily ascribed to the window-of-visibility theory.[12,30,37–39]

The window-of-visibility theory[37] attempts to account for perceived motion in complex patterns in terms of the Fourier composition of the stimulus pattern after filtering by the modulation transfer function of the human visual system. Components in the Fourier transform of the stimulus should have no influence on perception if their spatial and temporal frequencies are beyond the resolution limits of the visual system. Differences in attenuation of components within the window can affect the balance of Fourier energy in the filtered stimulus and as a consequence could influence perceived speed and direction of motion. Owing to the shape of the window of visibility, increasing the temporal frequency of a drifting stimulus may differentially attenuate the two moving sidebands of an amplitude-modulated grating [Figs. 1(a) and 1(b)] relative to each other. Since the envelope moves in the direction of the highest-spatial-frequency sideband, if its contrast is attenuated more than its lower-frequency counterpart, the imbalance will result in a bias in favor of the lower-spatial-frequency sideband. This may then cause motion to be perceived in the direction of that sideband motion which is opposite to that of the envelope.

D. Psychophysical Methods

1. Detection Thresholds

The experimental paradigm used to measure detection thresholds for the simple gratings and the noise carriers was a standard two-alternative forced-choice detection task. The stimulus was presented in one of two intervals, and the observer had to indicate by means of a mouse button press in which interval the stimulus had appeared. The contrast of the stimulus was adjusted by a modified staircase procedure[40] according to the observer's response. In both cases, noise and grating, the observer simply detected the first-order modulation, and the data presented therefore represents detection threshold only for a first-order-sensitive mechanism.[24]

2. Direction-Discrimination Thresholds

A two-alternative forced-choice direction-discrimination procedure was used to measure observers' ability to discriminate the direction of motion. In one of two intervals, chosen at random, the stimulus moved upward; in the other interval the stimulus moved downward. The observer had to indicate by means of a mouse button press in which interval the stimulus moved upward. The contrast of the carrier and depth of modulation of the envelope was scaled to the observers' ability to detect each respective aspect of the pattern. Details of each particular condition are given in the individual results subsections.

E. Contrast Scaling

It has become clear from much recent work that it is necessary to find some scaling factor by which to measure the contrast of the first-order carrier.[24] On the basis of this previous work, all the carriers in the current study are scaled to the observers' individual sensitivity for each condition. However, even with single-scale grating carriers this is not necessarily a straightforward issue, and this problem is amplified with multiple-scale noise carriers.[24,41] As well as considering these issues in light of the data, we use contrast as an independent variable within the study, which should overcome any serious problems that may arise from incorrect contrast scaling of the carrier. The contrast units quoted in the current paper are the peak contrast of the carrier (first-order) modulation.

3. RESULTS

This section deals with the results in the following manner. Given the number of figures needed to develop our argument, we will aim to describe each data set from each experiment carefully, bringing out the similarities and differences between observers. At the end of each experiment we will summarize the data and cast them in terms of our overall hypothesis. We have taken pains to bring out and experimentally examine any anomalies in the data before these general summaries. The general format for the majority of the figures is the same throughout and is given in Fig. 3(a) (below) and its caption. Vertically the graphs correspond to an observer as labeled; horizontally the carrier is either dynamic (i.e., updated at 25 Hz, top panels) or static (not updated, bottom panels).

A. Experiment 1: Detection Thresholds for Single- and Multiple-Component Carriers

Figure 2 shows detection thresholds of four observers for a range of carriers, plotted as a function of the spatial frequency of the fundamental in the carrier. Data for three of the four observers also include detection thresholds for single-grating carriers. The depth of envelope modulation was 0%, and all carriers appeared approximately uniform in contrast despite the modulation of contrast induced by the generation process.[42] Although there are slight differences in sensitivity among observers, the pattern of performance across carrier and fundamental frequency is approximately the same for all observers and is consistent with previous work.[41,43] These threshold measures provided a means of scaling stimuli at suprathreshold levels in subsequent experiments, providing for an equivalence between stimuli, when expressed in terms of units above threshold contrast, and between observers.

B. Experiment 2: Effect of the Carrier Format

Experiment 2 examines the basic anomaly within the published data that we would like to explain. At high temporal drift frequencies, the direction of motion of envelopes modulating single-grating carriers either cannot be discriminated or appears to reverse, whereas envelopes modulating multiple-scale carriers are seen to move forward, given sufficient contrast. It is this latter observation that stimulates the suggestion that the content of the carrier is critical to the ability to discriminate the motion of a contrast envelope and that motivates this work. This anomaly is addressed most simply by measuring observer's ability to discriminate the direction of motion of the contrast envelope as a function of the (scaled or un-

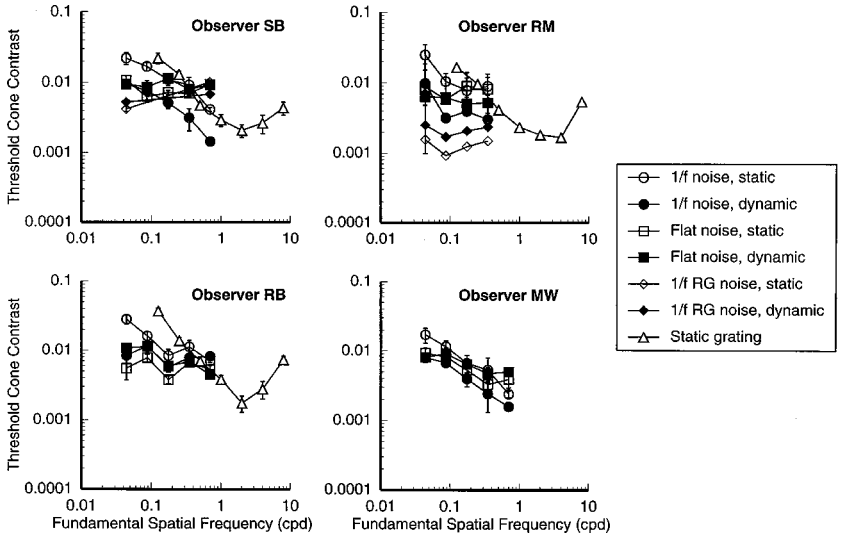

Fig. 2. Detection thresholds for grating and noise unmodulated carriers. Mean L–M-cone contrast is plotted against the spatial frequency of the fundamental in the noise (or of the grating). The format of the carrier is indicated in the legend. Data for four observers is shown, one observer per panel. Stimuli were presented in a two-alternative forced-choice detection paradigm within a 20° disk and a raised-cosine temporal envelope, the half-width of which was 500 ms.

scaled) contrast of four different kinds of carrier: a single sinusoidal grating (0.724 cpd), binary noise, flat grayscale noise, and 1/*f* noise.

As the aim of this experiment is principally to highlight the issue at hand, data are presented for two observers only (SJC and RM) as a function of contrast (SJC) and temporal drift frequency (RM); all conditions are replicated in further experiments. To aid comparison with previous work and span different units of contrast scaling, data for SJC are plotted in terms of Michelson contrast. All subsequent data are plotted in terms of multiples of contrast threshold as measured in the Experiment 1. The detection threshold for SJC for the noise carriers (0.044-cpd fundamental) is approximately 0.01 for the dynamic carrier and 0.03 for the static carrier giving a minimum contrast of 20× and 6.67× threshold, respectively. Within each graph the different noise formats are indicated by different symbols, and data are presented for both static (not updated) and dynamic (updated every three frames, 25 Hz) noise. This static versus dynamic terminology is adopted throughout the paper. In the single-grating carrier condition, the phase of the carrier was randomly reassigned every three frames to equate the dynamic properties of this carrier to the dynamic properties of an equivalent component in the composite noise image. We note at this point that the rate of update of the carrier does not affect the data significantly; the only difference, for example, between a 75-Hz update rate and 25-Hz update rate is a reduction in the perceived reversal.

Figure 3 (SJC) compares all three noise formats and the grating carrier, plotting the perceived direction of the same 0.182-cpd, 100% modulation in the carrier contrast as a function of the carrier (peak) contrast. Data for two temporal frequencies are displayed, 2 Hz (solid symbols) and 16 Hz (open symbols). Dynamic carriers, updated at 25 Hz, are plotted in the top panel, and static (not updated) carriers are plotted in the bottom panel. This is

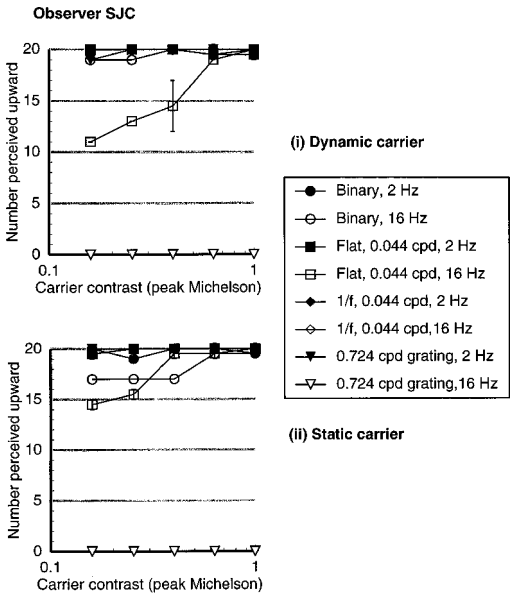

Fig. 3. Envelope direction-discrimination with different carrier types as a function of contrast for observer SJC. The perceived direction of envelope motion is plotted against the carrier (Michelson) contrast for low (2-Hz) and high (16-Hz) temporal envelope drift rates to illustrate the basic discrepancy in the data motivating the study. Top panel, data for a dynamic (updated at 25 Hz) carrier; bottom panel, data for a static (not-updated) carrier; additionally denoted (i) and (ii). There were at least 40 observations per point, and the error bars are ± standard error of the mean (also in all subsequent figures). Symbols denoting different carrier types are indicated in the legend. Fundamental in the noise, 0.044 cpd; spatial frequency of the envelope, 0.2 cpd; 100% modulation. This general format (with differences between the *x* axes and symbols and observers) is followed throughout the paper.

the case throughout the paper unless otherwise stated, although symbol allocation does alter between experiments.

At the low temporal drift frequency of 2 Hz (solid symbols), the direction of motion can be discriminated per-

fectly at all noise and grating carrier contrasts and with both dynamic and static carriers. At a high temporal drift frequency of 16 Hz, the percept is somewhat degraded, particularly when the carrier is dynamic flat noise, in which case a higher contrast is required to accurately discriminate direction. The data with the noise carriers reflect what has previously been shown for high-contrast, high-temporal-frequency contrast-modulated noise stimuli,[44] although in previous cases the noise has been binary and two dimensional.

The data for the high-temporal-frequency (16-Hz) grating carrier shows a complete reversal in both dynamic and static conditions; i.e., the stimulus is seen to be moving in the direction opposite to that of the envelope. This anomalous result has been shown before (Refs. 12 and 34, but see Ref. 45) and is most intuitively explained in terms of the theory of the window of visibility[37] as outlined in Section 2.

Figure 4 presents data for the different types of noise carrier. Perceived direction is plotted against the temporal drift frequency of the envelope (observer RM). The peak contrast in the carrier was set at 1.5 log units above threshold for the carrier alone, which is a peak Michelson contrast of approximately 0.93 for this observer. The three kinds of noise carrier are binary, flat gray-scale, and 1/*f*, as in Fig. 3.

At lower temporal drift frequencies, direction-discrimination performance is close to perfect for all carriers in both static and dynamic conditions. As the temporal frequency rises above 8 Hz, there is a moderate dip in the ability to discriminate direction for the flat gray-scale and 1/*f* carriers. This effect is more pronounced for the gray-scale noise carriers (squares) and reaches a minimum of chance performance at ~12 Hz. These data are reminiscent of the bimodal function of direction discrimination against temporal frequency shown for beat patterns.[46] By the maximum drift frequency of 16 Hz, performance for all noise-carrier stimuli recovers to give the correct perceived drift direction. In the static noise-carrier condition performance is less variable with temporal frequency; only a moderate drop in discrimination is seen at the highest temporal frequency. It is worth noting that any staircase procedure for measuring performance (set to give threshold at 75%, as many are) would still register this as veridical motion perception; performance stays above 75% correct. The data for the same contrast envelope but a grating carrier (triangles) is completely different. As temporal frequency increases, performance changes from ~100% correct to ~100% incorrect (reversed motion) by a temporal drift frequency of 10-Hz (dynamic) or 6 Hz (static).

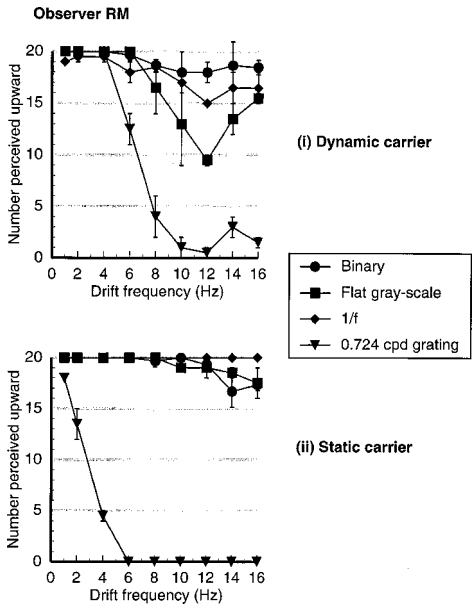

Fig. 4. Envelope direction discrimination with different carrier types as a function of temporal frequency for observer RM. The perceived envelope direction is plotted against the temporal drift frequency of the 0.2-cpd envelope. The carrier contrast was 1.5 log units above detection threshold (Michelson peak ~0.93) with a fundamental of 0.044 cpd. Other details as in Fig. 3.

Why then is there such a drastic change in perceived direction induced simply by changing the carrier? The drifting contrast envelope to which the observer is responding is exactly the same for all stimuli. We suspect that the lack of reversal seen in the 16-Hz data for noise carriers reflects the presence of low-spatial-frequency components in the noise. The remainder of the paper examines this issue by investigating the effect of changing a carrier systematically from a simple grating to a compound noise carrier on performance. This will allow us to test the theory that the window of visibility is critical in determining the perceived direction of motion for these types of stimuli.

C. Experiment 3: Effect of Fundamental Frequency

A. Experiment 3a: Carrier Contrast

Probably the most critical aspect of changing a carrier from a grating to a noise carrier is the change from a single-scale to a multiple-scale luminance modulation. Experiment 3 investigates this experimentally by gradually changing the carrier fundamental while examining observers' ability to discriminate motion in a contrast envelope that remains at a constant modulation depth and frequency across all stimuli. The fundamental frequency of a binary-noise carrier cannot be easily and reliably controlled. Any filtering process will introduce gray scale into its representation. There is little expectation, however, for the behavior elicited to a binary carrier to be significantly different from that for a gray-scale noise carrier.

Figures 5(a) and 5(b) present data pertaining to the effect of carrier contrast on the perceived envelope direction at high and low temporal drift frequencies (2 Hz, solid symbols; 16 Hz, open symbols) the fundamental frequency of a flat (gray-scale) noise carrier is changed from 0.044 to 0.724 cpd. Each figure part presents data from a different observer. Figure 5(a) plots the direction-discrimination performance against the peak Michelson contrast for observer SJC; Fig. 5(b) plots the contrast in threshold multiples for observers MW and RM.

Open symbols indicate the conditions in which we suggest there is some issue about whether low spatial frequencies in the carrier may be mediating the discrimination of motion in these stimuli (i.e., at a high temporal drift rate of 16 Hz). Solid symbols represent a low tem-

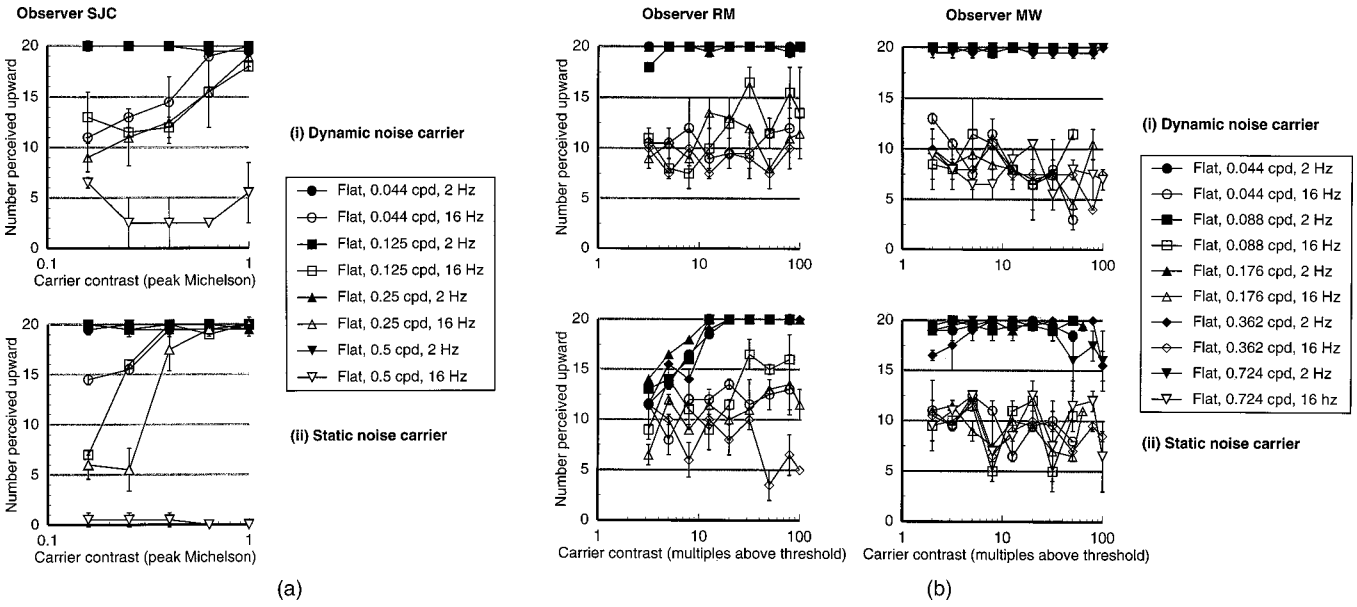

Fig. 5. Envelope direction discrimination for one-dimensional flat (gray-scale) noise carriers to examine the effect of increasing the fundamental in the noise. The perceived direction of envelope motion is plotted against the carrier contrast [(a) Michelson, SJC; (b) threshold multiples, RM and MW] for low (solid symbols, 2 Hz) and high (open symbols, 16 Hz) temporal drift rates. The fundamental is progressively increased as indicated in the legend. Open symbols, conditions in which the fundamental is at a higher spatial frequency than the envelope (0.2 cpd). Carrier contrast is 1.5 log units above threshold for observers RM and MW.

poral drift rate of 2 Hz, where it is clear that we can discriminate contrast-coded motion whatever the spatial frequency content of the carrier; see, e.g., Refs. 7, 14, 47, and 48.

At the low temporal drift rate of 2 Hz (solid symbols) the fundamental frequency of the carrier has little or no effect on the perceived direction of motion, which is consistently between chance (50%) and 100% correct for all observers regardless of contrast scaling. The moderate (peak) carrier contrast of 0.2 [minimum for SJC, Fig. 10(a) below] is more than enough to elicit 100% correct performance and indeed is twice detection threshold in the majority of cases for the other observers. These data agree specifically with those collected with grating carriers.[33]

At the high temporal drift rate (16 Hz) the effect of the fundamental frequency is seen most clearly for SJC (scaled in terms of Michelson contrast), although there is a suggestion of an effect across the other observers. Principally, the motion becomes much harder to discriminate across all fundamental frequencies, and performance only rises above 75% correct (upper horizontal division on figures) at much higher contrasts (0.6–0.7). For the fundamental frequencies lower than, or similar to, the envelope modulation frequency (0.2 cpd), which appears to include a 0.25-cpd fundamental as an upper limit (SJC), the perceived direction of motion is forward. For the higher fundamental frequencies (>0.25 cpd) the perceived direction of motion is reversed, and the point at which performance moves outside the range of chance (25%–75%) is at a lower contrast (0.25). For the other observers the data are inconclusive apart from the fact that motion is much harder, if not impossible, to discriminate in many cases, and where there is an effect of the fundamental the data are consistent with the data of SJC [e.g., Fig. 5(b), RM static carrier]. Changing the carrier from dynamic to static tends to have the effect of increasing the percept of motion, whether that be forward or reversed. This is again most obvious for observer SJC.

Figures 6(a)–6(c) present data for the same conditions as in Figs. 5(a)–5(c) except that the carrier had a $1/f$ noise format. All cited thresholds are for this type of carrier. The data show much the same pattern of results as for the flat carrier except that the effects are much clearer. Figure 6(a) plots Michelson contrast against performance in the direction-discrimination task for observer SJC. Figures 6(b) and 6(c) plot contrast in threshold units against performance for three other observers. The majority of figures show the same trend in performance: performance is close to perfect for the slow (2-Hz) drift rate as a function of contrast and fundamental frequency, and performance changes from forward to reverse motion for the fast (16-Hz) drift rate as a function of increasing fundamental frequency. Generally, performance in the higher-drift-rate condition also requires a higher contrast for a given (forward or reverse) performance level. Changing the carrier from dynamic to static tends to increase the degree of reversed motion perceived at high drift rates.

There are a couple of important anomalies worth mentioning. In the static carrier condition, observer SJC tends to see more forward motion even at higher fundamental frequencies than the other observers but remains strongly reversed in the critical 0.5-cpd fundamental condition. Again in the static condition, observers RB and RM seem to have difficulty perceiving motion in the slow-drift-rate condition with the highest fundamental frequency. Observer reports suggest that induced motion in the carrier causes two directions to be perceived; this effect will be explicitly examined in Experiment 4c.

To summarize the results of Experiment 3a, slow drift rates are generally unaffected by changing the carrier

fundamental frequency, whereas the perception at high drift rates is strongly affected by such a manipulation, which changes the perceived motion from forward to reversed as fundamental frequency rises above that of the envelope. The effect is exacerbated with 1/*f* noise carriers and particularly when they are not updated. In the context of our hypothesis, we can explain the reversal at high temporal frequency for single-component carriers by proposing that the highest-spatial-frequency component falls outside, or at least is more attenuated by the window of visibility.[37] For broadband noise there is some component energy in the envelope direction, which one assumes is balanced by energy in the opposite direction[13]; however, in this case the visual system can still recover envelope motion. For high-pass noise carriers there is an imbalance in the Fourier spectrum similar to that with grating carriers, which, when considered in relation to the window of visibility, means that motion may be seen in the reversed direction. The only difference between the two situations, yielding forward motion on the one hand (unfiltered) and reversed motion on the other (high-pass filtered), is the low-spatial-frequency content of the carrier.

B. Experiment 3b: Carrier Drift Frequency

Experiment 3b examines the effect of changing the temporal drift frequency of the contrast envelope at a set carrier contrast (+1.5 log units as denoted in the figures, Michelson peak near 0.93 depending on the observer). Figures 7(a)–7(d) plot the performance in the direction-discrimination task as a function of temporal drift frequency of the contrast envelope. Given that the data are clearer for a 1/*f* carrier format and that the empirical relationship between flat and 1/*f* carriers has been shown in Experiment 3a, only one full example of a flat carrier is presented in this experiment [observer RM, Fig. 7(a), and

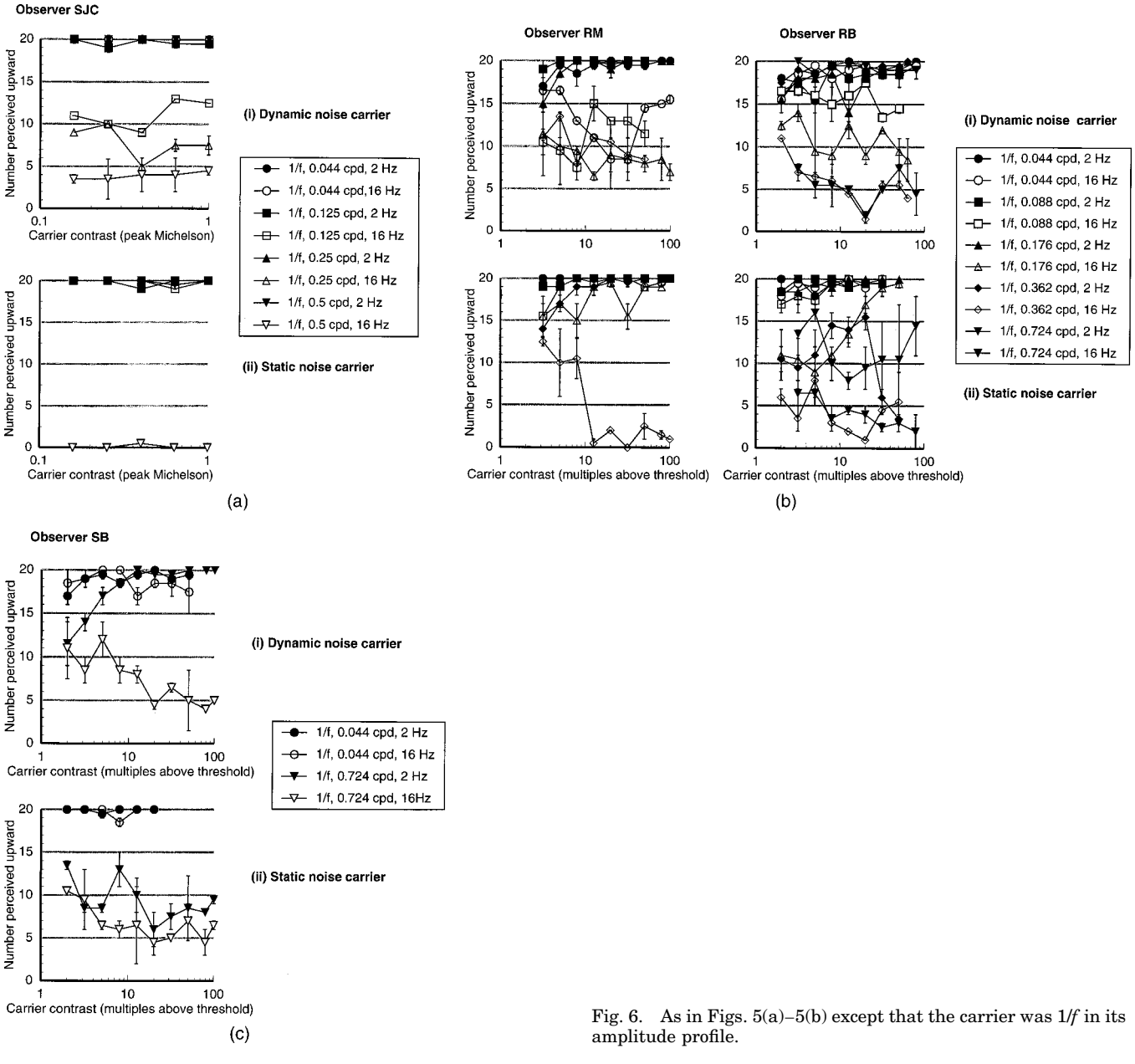

Fig. 6. As in Figs. 5(a)–5(b) except that the carrier was 1/*f* in its amplitude profile.

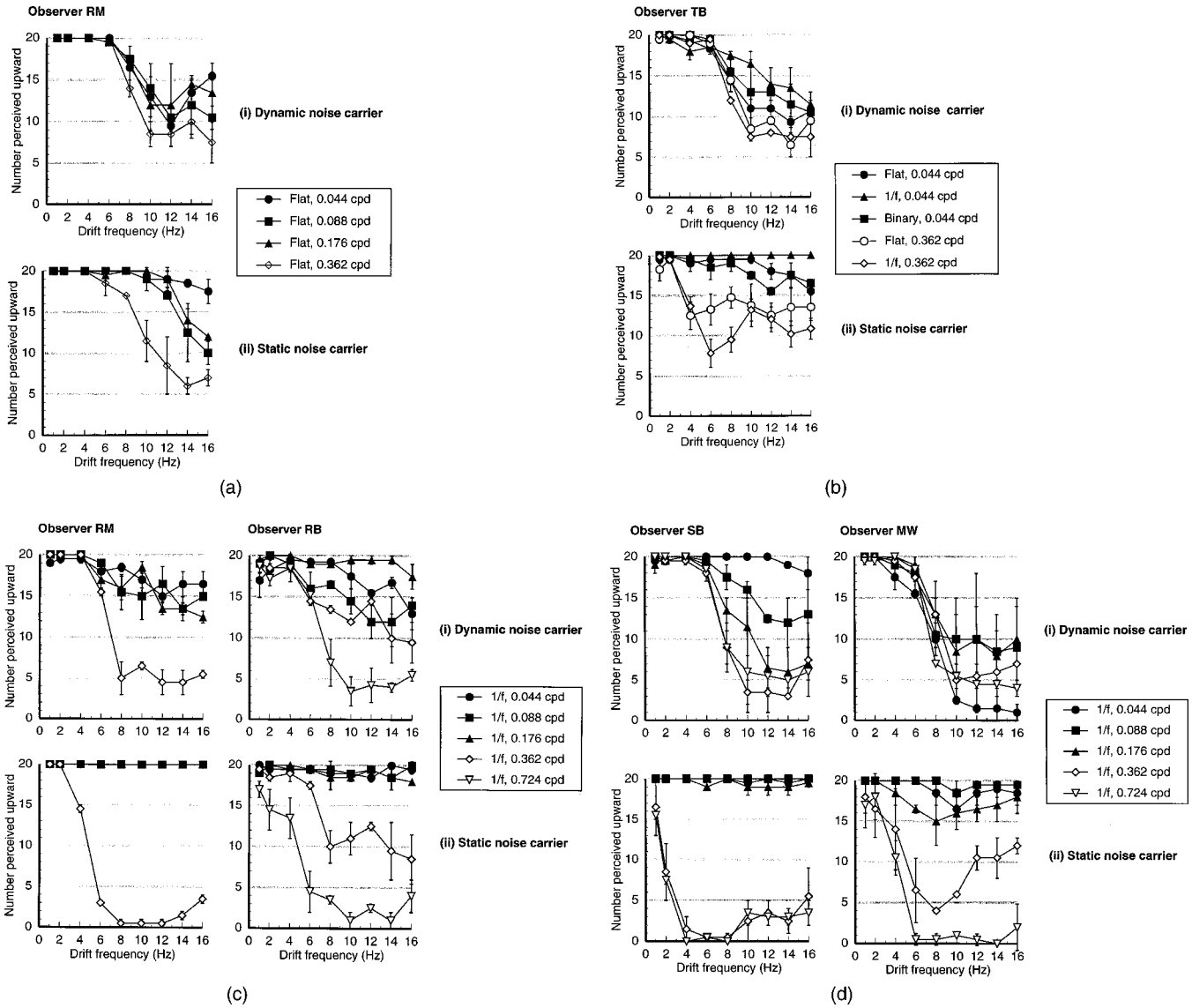

Fig. 7. Similar to Figs. 5(a) and 5(b) except that the independent variable plotted on the x axis is temporal drift frequency. The carrier contrast was set at 1.5 log units above detection threshold for all observers, and the amplitude spectra were either flat [(a) RM, (b) TB] or had a $1/f$ profile with respect to spatial frequency [(c), (d)]. Other details as in Fig. 3.

reduced conditions for observer TB, Fig. 7(b)]. Furthermore, these reduced conditions show that the effect of changing the noise format is the same as shown in Experiment 3a: The differences in performance across temporal frequency are greater for $1/f$ noise. To clarify the presentation of this data in terms of our hypothesis, stimuli where the carrier has a higher fundamental frequency than the envelope have open symbols; stimuli where the fundamental is at a lower frequency, i.e., conditions that we suggest contain oriented low-spatial-frequency modulation, have solid symbols.

Examination of all of Fig. 7 (flat and $1/f$ carriers) reveals that at low temporal drift rates up to ~6 Hz, performance is close to perfect in the discrimination task for all fundamental frequencies. As the temporal drift rate increases, the effect of fundamental frequency becomes obvious such that veridical performance remains at a reasonable level for the conditions where the fundamental is below the envelope frequency; once the fundamental rises above 0.2 cpd, performance drops to chance or below, where a reversal is seen. Not updating the carrier tends to exacerbate this effect, the most clear example of which is shown in Fig. 7(c) (observer RM, $1/f$ noise). Again there are some anomalies to this generalized description; observers RB and SB both show a strong reversal even at lower temporal frequencies in the static condition [Figs. 7(c) and 7(d), respectively], and observer TB drops to chance with no reversal in the higher fundamental condition for both types of carrier [Fig. 7(b)]. Observer MW, in the dynamic condition [Fig. 7(d)], shows a strong reversal for the 0.044-cpd condition at higher temporal frequencies and poor (chance) performance for the other fundamental frequencies. His data revert to the predicted pattern in the static condition. For this observer we examined whether the extent (size) of the stimulus was having an effect on the reversal as is the case for single grating carriers.[34] This is shown in Fig. 8, where data for the highest (0.724-cpd) and lowest (0.044-cpd) fundamental

conditions are presented when the stimulus is displayed in a 4° disk (small symbols) rather than a 20° disk (large symbols, data shown for comparison). The reversal in the dynamic condition is removed and performance reverts to chance. This observer, however, still does not see forward motion in this condition (0.044-cpd higher temporal frequencies). Interestingly, in the 0.724-cpd condition there is also some forward motion indicated at the highest temporal frequencies, although performance is notably worse than that measured for temporal drifts below 6 Hz. This kind of observer variability is not unusual in the data, and all data are included to demonstrate the degree of variability to be expected with these types of stimuli.

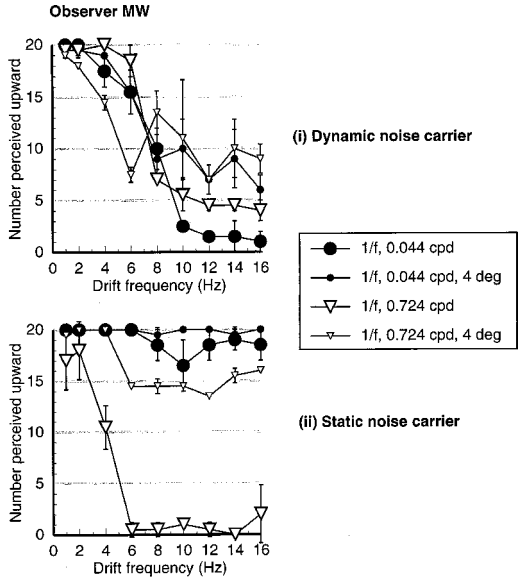

Fig. 8. As in Fig. 7(d) except that the stimulus was restricted to a 4° centrally located window. Small symbols indicate this condition; large symbols are the 20° condition replicated from Fig. 7(d).

The effect of stimulus size is examined in more detail elsewhere,[34] but a very strong reversal is seen across all observers when an envelope is drifted rapidly across single grating carrier in a centrally placed 20°/8° annulus.[34]

In summary, once the possibility of modulation-induced components in the envelope direction is reduced by increasing the fundamental frequency in the carrier, denoted by the open symbols, there is little evidence for correct perceived motion at drift frequencies above around 6 Hz even at the maximum available stimulus contrast. In many cases there is also a strong reversal, which indicates a further dependence on the Fourier composition of the stimulus.

Finally, since it has been argued that there is no significant difference between chromatic and luminance carriers in the perception of contrast-coded motion,[33,34,49] Figs. 9(a) and 9(b) present data for a 1/*f* red–green carrier modulated by a 0.2-cpd contrast envelope as a function of that envelope's drift frequency. The contrast is 1.3 log units above threshold for detection of the carrier alone, the maximum available for each observer. Other conditions are the same as for the luminance carrier. There is no significant difference between the data presented for the red–green carrier and that presented for the luminance carrier. The only possible difference is that with the higher-frequency carriers in the updated condition, there seems to be a reduction in performance at the lower temporal frequencies. Even though the contrasts are scaled by the detectability of each carrier, this reduction may not be so surprising considering the reduced temporal sensitivity of chromatic detection mechanisms[48,50,51] and the additional temporal frequencies introduced into the neural image by the updating of the carrier.

In summary, Experiment 3 shows that for dynamic noise carriers with a fundamental frequency that is lower than the envelope frequency (solid symbols), the high temporal frequencies generally require higher carrier

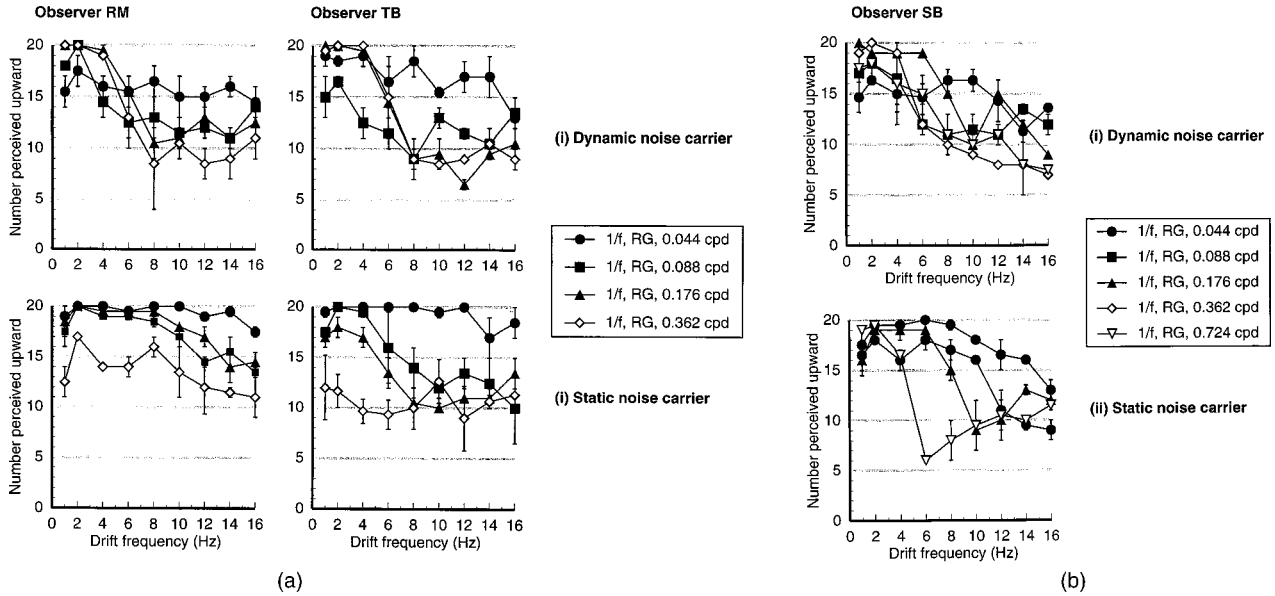

Fig. 9. Direction discrimination for an envelope (0.2 cpd) modulating a 1/*f* red–green noise carrier as fundamental carrier frequency increases. The perceived direction of envelope motion is plotted against the temporal drift frequency. The carrier contrast was set at a maximum of 1.3 log units above detection threshold for the three observers. Other details as in previous figures.

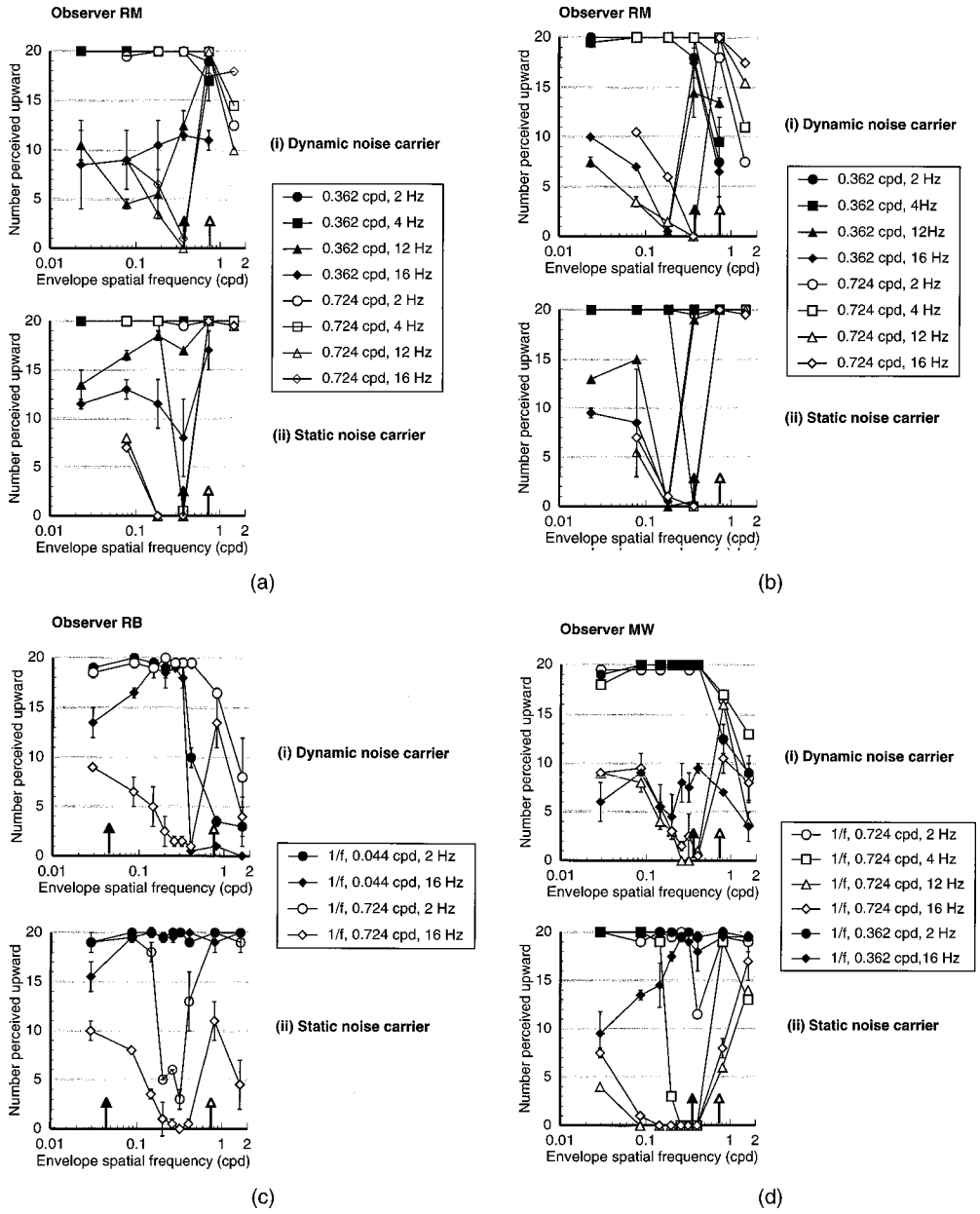

Fig. 10. (a) Envelope direction discrimination as a function of envelope spatial frequency for a fixed fundamental frequency. Temporal drift frequency and carrier fundamental spatial frequency are indicated in the legend. Arrows on the x axis indicate the fundamental frequencies of the carriers. Open and solid arrowheads relate to open and solid symbols. (a) Data for a flat noise carrier at a contrast of 1.5 log units above threshold for observer RM. (b)–(d) As (a) except that the carrier has $1/f$ noise profile.

contrasts. For dynamic noise carriers with a fundamental frequency that is higher than the envelope frequency, at high temporal frequencies only, motion is seen in the direction opposite to that of the envelope motion if directionally consistent motion is at all discriminable. Again, given our hypothesis, we suggest that in the case of amplitude-modulated gratings it is possible to identify a component in the direction opposite to that of motion: the lower sideband. However, in the case of contrast-modulated noise carriers, unlike with grating carriers, we cannot attribute reversed motion to a particular component; rather, we can attribute the reversal to the relative reduction of components in quadrants that relate to envelope motion, thus creating an imbalance that results in the reversal.

D. Experiment 4: Further Examination of Carrier Dependence

A. Experiment 4a: Manipulation of Envelope Spatial Frequency

Given our theory, the envelope spatial frequency is an obvious independent variable, to manipulate. It is worth noting at this juncture that observer RM also replicated the whole of his data (not shown) presented in Experiments 2 and 3 with a 0.1-cpd envelope with no significant differences in performance across any of the conditions. Figures 10(a)–10(d) present data for three observers (RM, RB, and MW), where the fundamental carrier frequency was kept constant and the envelope frequency varied as plotted on the x axis. Figures 10(a) and 10(b) present

data for RM for flat and 1/*f* noise, respectively. Figures 10(c) and 10(d) present data for observers RB and MW, respectively, for 1/*f* noise. Temporal drift frequency and fundamental spatial frequency of the noise carrier are indicated in the legend. The arrows on the *x* axis indicate the envelope spatial frequencies at which we propose that low-spatial-frequency components may be significant (envelope spatial frequency ⩾ fundamental spatial frequency), and if this is the case the perceived direction of motion is more likely to be forward (correct), particularly at high temporal frequencies. Open and solid arrowheads relate to open and solid symbols for the fundamental frequency as denoted in the legend.

Although the data are a little noisy, the principal effect is that at higher temporal frequencies it is not until the envelope spatial frequency rises above the fundamental spatial frequency that veridical motion is seen in the stimulus. When the envelope spatial frequency is lower than the fundamental spatial frequency and is drifting at 16 Hz, there is a strong reversal, consistent with our observations and theory thus far—i.e., a dependence on the Fourier components in the stimulus. At the lower temporal drift frequencies, increasing the envelope spatial frequency above that of the fundamental tends to have a detrimental effect on direction discrimination in the dynamic condition. This is most pronounced in the updated carrier condition with observer RB [Fig. 10(c)], even showing quite a strong reversal in the 2-Hz/0.044-cpd condition. One major peculiarity in the data is the reversal seen for observers RM and MW in the static carrier condition at a drift rate of 4 Hz and a carrier fundamental of 0.724 cpd. This finding is expanded on in Experiment 4c.

B. Experiment 4b: Reduction of Stimulus Duration

It has been shown both directly and indirectly that there is some critical period below which the motion of a contrast modulation cannot be discriminated.[12,33,48,52] Experiment 4b utilizes this fact by reducing the duration of the stimulus to 107 ms, which is approximately the lower limit for contrast-modulated motion detection. If the direction-discrimination performance reflects the presence of a component moving in the envelope direction induced by the modulation of a low-spatial-frequency component, then we should see little or no effect on direction discrimination by this manipulation, because motion of a luminance modulation can be discriminated at a duration as short as 15 ms[48] as long as it is moving fast enough.

Figures 11(a) and 11(b) present data for observers RB and MW, respectively, plotting the number perceived upward as a function of the temporal drift frequency of the envelope. Static and updated 1/*f* carriers are shown as in previous figures, and the different symbols relate to different fundamental frequencies. The carrier contrast is 1.5 log units above threshold. The comparison graph for RB is Fig. 7(d), where the stimuli were presented for the standard duration of 500 ms. The 500-ms data are shown on the figure for observer MW [Fig. 11(b)]. As in previous figures, open symbols indicate a stimulus where we consider there to be no luminance component moving in the envelope direction. The data for observer RB are fairly conclusive in that as soon as the envelope frequency rises above the carrier fundamental (open symbols), the performance in the motion task drops to chance for all temporal frequencies measured. Observer MW again shows more variability in that there is a moderate degree of forward motion seen at 8 Hz in the 107-ms, 0.724-cpd condition. At the higher temporal frequencies there is a clear difference between the short- and long-duration data. In addition to removing the forward-motion percept in the 0.044-cpd condition, reducing the duration removes the reversal in the static 0.724-cpd fundamental condition seen for both observers. MW also showed a reversal in the 0.044-cpd long-duration condition [see also Fig. 7(d)], which as well as being removed by a reduction

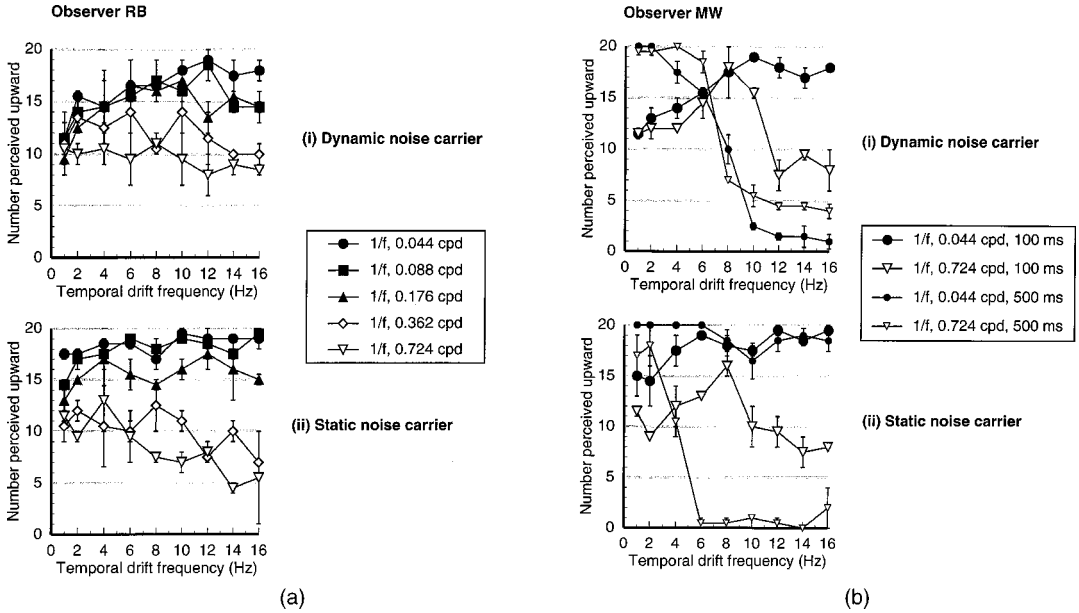

Fig. 11. Envelope direction discrimination plotted against temporal drift rate at a reduced stimulus duration of 107 ms for a 1/*f* noise profile. All other conditions are the same as Fig. 7(c), which should be examined for comparison for observer RM. Reduced conditions allow comparison (500 ms) data to be included for observer MW in (b) [see also Fig. 7(d)].

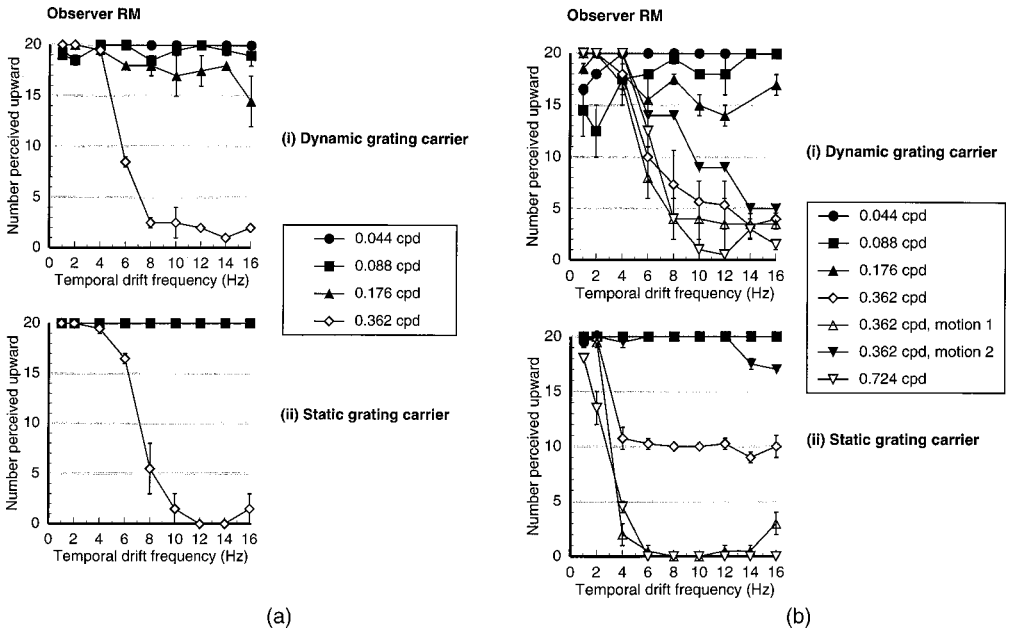

Fig. 12. Envelope direction discrimination as a function of temporal drift frequency for the fundamental alone. Details the same as Fig. 7(c), which should be taken as the comparison figure for observer RM. (a) Carrier contrast 1.5 log units above threshold for a 1/*f* noise carrier of the same fundamental spatial frequency. (b) Carrier contrast 0.3 log unit above threshold. See text for an explanation of the 0.362-cpd plots.

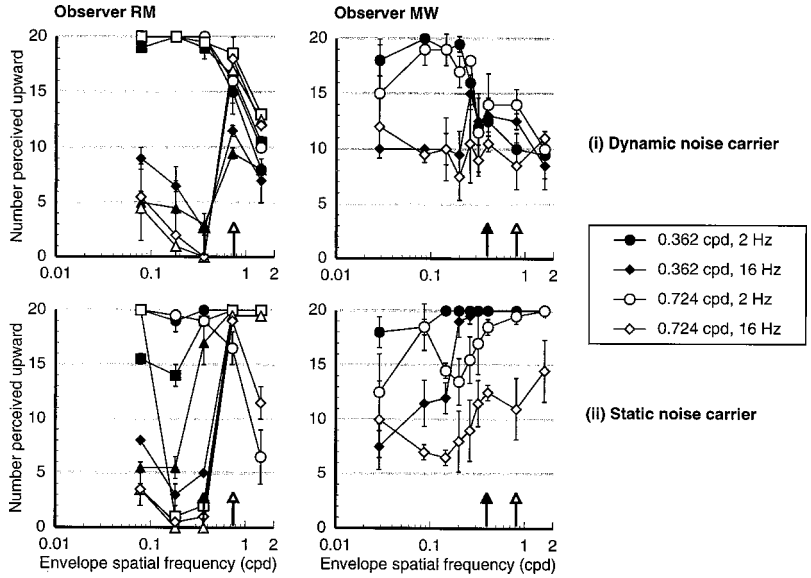

Fig. 13. Direction discrimination as a function of envelope spatial frequency for a fixed fundamental frequency. Fundamental alone at a contrast of 0.3 log unit above detection threshold for the 1/*f* noise profile. As a comparison figure, and for other details, see Figs. 10(b) (RM) and 10(d) (MW).

in stimulus spatial extent (Fig. 8) is now removed by a reduction in duration. In this case however the percept reverts to a strong forward motion. This implies that although the forward motion may be due to oriented Fourier components in the stimulus in line with our hypothesis, the reversal seen in this condition for this observer may be due to induced motion in the carrier[53] that is a product of something more than simply the distribution of stimulus components.[34]

In summary, the general reduction in performance supports our hypothesis with respect to the effect of low spatial frequencies in the carrier and also is in agreement with previous work that claims that motion in a contrast envelope cannot be discriminated accurately below ~100 ms. Our hypothesis is, of course, supported only if we accept the conclusions of this previous work.

C. Experiment 4c: Can These Data Be Explained by the Fundamental Component Alone?

In a noise carrier, each component is at a relatively low contrast even when the noise itself is at a high contrast. Thus it is possible that the components in question, i.e., those below the frequency of the envelope modulation, may not actually be detectable and may therefore not be

instrumental in mediating the observer's performance. The current experiment examines this suggestion by using the fundamental of the noise stimulus as the carrier: a simple grating at the fundamental frequency. For continuity, however, it is constructed and presented in exactly the same way as the noise carrier. In the updated condition, therefore, the grating is randomly repositioned at each update.

Figures 12(a) and 12(b) present data for observer RM at high [+1.5, Fig. 12(a)] and low [+0.3, Fig. 12(b)] fundamental contrasts. The direction discrimination is plotted against the temporal drift frequency of the envelope for four different fundamental frequencies, as denoted by the different symbols. Open symbols indicate a condition in which the fundamental is higher in spatial frequency than the envelope. These figures should be compared with Figs. 7(a) (flat noise) and 7(c) (1/*f* noise) for the same observer (RM).

In the higher-contrast condition the data are very clear. At low temporal frequencies, performance is perfect; at drift rates higher than 4 Hz there is a strong reversal in the condition in which we suggest that no component is moving in the envelope direction generated by contrast modulation that may mediate correct (forward) direction discrimination. This is the case in both dynamic and static conditions. In the former, stimulus-carrier phase is randomly updated every three frames (every 40 ms). Motion discrimination still remains very good despite this additional noise, which is also likely to be detectable by the motion system.

The contrast of the fundamental in the noise stimulus will be much lower than 1.5 log units above threshold, so the data for a carrier 0.3 log unit above threshold is presented in Fig. 12(b). This is the lowest carrier contrast at which envelope motion may be adequately seen.[33] The data in Fig. 12(b) are basically the same as that presented in Fig. 12(a), apart from two differences. First, the data are generally far more inconsistent and noisy although showing the same trend and effect of fundamental frequency; second, there is one condition (0.362-cpd fundamental) in which two motions are clearly visible to the observer. What is more, the observer is able to clearly discriminate between the two and report either direction at will. This is indicated by the curves for the 0.362-cpd fundamental. The triangles show the performance when the observer was instructed to respond to either one perceived direction or to the other; the observer was experienced and able to apply this criterion consistently. The diamonds show the means of these two data sets for the static condition and for the initial data collected in the dynamic condition, when the observer was essentially naïve to the possibility that two motions might be visible, i.e., before the observer reported the ambiguity. Although this is a slightly odd result, it does fall into line with the strong reversal that was seen in some of the previous data [e.g., RM, Fig. 10(c), 2 Hz/0.044 cpd] and that we ascribe to induced motion in the carrier grating under particular (close) carrier-to-envelope frequency relationships.[53]

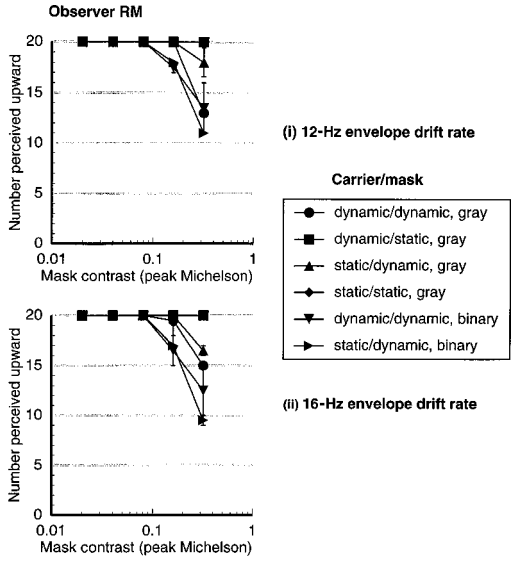

Fig. 14. Envelope direction discrimination for the fundamental alone (0.044 cpd, 0.3 log unit above threshold) with a noise mask superimposed on the stimulus. Perceived direction is plotted against the Michelson (peak) contrast of the noise mask. The mask may be static or dynamic and had a flat (gray-scale or binary) amplitude profile. Upper panel, drift rate of 12 Hz; lower panel, drift rate of 16 Hz.

It is pertinent to note, when one is considering the window-of-visibility theory, that the three components of the amplitude-modulated grating created by this combination are equally spaced along the spatial frequency axis (0.18 cpd, 0.36 cpd, 0.54 cpd). If the observer were able to discriminate among these three components, which is a possibility given their frequency relationship and early visual filtering,[54] the two sidebands might contribute equally to the motion percept and also be discriminable on that basis. The aspect of the motion detection system under attentional control has an obvious role in this result, although the degree of attentional tracking *per se* is difficult to ascertain.[55]

The effect of the envelope spatial frequency at a fixed fundamental frequency is shown in Fig. 13 for observers RM and MW. This is a replication of Experiment 4a with use of a single grating (fundamental) carrier rather than a noise profile. The comparison figures for observer RM are Figs. 10(a) and 10(b) and for observer MW Fig. 10(d). The data are essentially very similar. At higher temporal frequencies, forward motion (or a reduction of the reversal to chance performance) is seen only when the envelope frequency rises above that of the fundamental.

The conclusion from the presentation of the fundamental alone is that the data can largely be explained on the basis of this component of the stimulus. The dynamic condition suggests that the common manipulation of updating the carrier may be useful only if refreshed each time the envelope itself is displaced. It is apparent in the data that updating the carrier does have some effect on envelope direction discrimination, particularly at higher temporal frequencies. This effect is examined in Experiment 4d.

D. Experiment 4d: Masking the Fundamental

It has been previously argued that updating the underlying carrier is sufficient to remove any first-order artifact in the stimulus,[2,4,6] but, as discussed in Section 2, stimuli with dynamic carriers are subject to the same concerns with respect to the influence of low spatial frequencies in

the carrier on perceived direction of motion. In addition, the dynamic nondirectional motion of the carrier may serve to mask or interfere with the extraction of envelope motion however that may be performed.

Figure 14 plots the perceived direction of a 0.2-cpd envelope in a fundamental-only grating carrier for two (high) temporal frequencies as indicated on the figures (12 Hz, top; 16 Hz, bottom) plotted against the contrast of a noise mask. Each curve is a different masking condition where either or both the carrier and the superimposed (temporally and spatially contingent) mask may be updated or static within the presentation interval. The masks are flat gray-scale noise or binary noise at the contrast indicated on the *x* axis. The contrast of the fundamental was at a very low contrast of 0.3 log unit above detection threshold, as for Fig. 13.

The data for both temporal frequencies are similar. The static mask has no effect on performance in either condition at any contrast. When the mask is updated, however, there is a reduction on performance as the mask contrast increases. The greatest reduction is seen for a binary mask whether the carrier (stimulus) fundamental is updated (dynamic/dynamic) or not (static/dynamic). This finding is consistent with the reduction in performance seen in previous work where the (usually binary) carrier is updated, and it may be explained as a moderate masking of the envelope motion.

4. DISCUSSION AND CONCLUSIONS

Although the idea of the visual system as a Fourier analyzer is now outdated, Fourier analysis techniques provide an important way of understanding the properties of moving stimuli and how manipulations mediated by neural mechanisms may influence visual perception. Second-order or non-Fourier stimuli have provided a challenge to linear-systems approaches to motion analysis since the spatiotemporal frequency description of these stimuli offers no immediate clues as to how the motion of contrast envelopes is recovered. Models can be classified as correspondence based[56,57] or spatiotemporal-gradient based.[58] A principal difference between these two models is that only the spatiotemporal-gradient model needs a temporal analysis of the input for performance of its calculations; a simple delay independent of the input will suffice for the correspondence-based detector. This point concerns the principals of motion extraction inherent in each of the two models and must not be confused with the implementation of either model type.

Recovery of the motion of a second-order spatial modulation is thought to be either an emergent property of standard spatiotemporal gradient motion analysis[53,59] or dependent on a supplementary mechanism specialized for this type of motion stimulus.[14,28,47]

If the detection of contrast modulation reflects an emergent property of local spatiotemporal-gradient analysis, carrier dependent effects are to be expected, since in this approach there is no attempt to extract or reconstruct the envelope modulation from the compound stimulus. The motion direction seen is a result of the shaping of the spatiotemporal-image's intensity surface by the interaction of modulation and carrier.[25] On the other hand, if there is a special mechanism for the extraction and analysis of the modulation, carrier dependent effects can be interpreted only as resulting from deficiencies in this mechanism or as an interaction between different motion-processing modules. An ideal envelope-extraction mechanism should be unaffected by the nature of the carrier, so long as the carrier is detectable.[14,28]

The experiments detailed above have shown that manipulating the carrier while keeping the envelope constant can have profound effects on perception of motion direction, and we suggest that we can best understand the perceived direction of motion in these stimuli as an interaction between neural filtering of the stimulus and the sensitivity of the visual system to the spatiotemporal frequency components in the filtered stimulus. Note that the filtering operations considered in the frequency domain will have their complementary effects in the image domain.

We found that observers are unable to correctly determine the direction of motion of a contrast envelope at temporal frequencies above approximately 4–6 Hz. This finding is consistent with some previous data[12,33,34,60] and in conflict with others.[14,19,45,46,61,62] The prevailing difference between these two sets of results is that the majority of the data showing an ability to correctly discriminate direction of motion at higher temporal frequencies used noise carriers (except Refs. 45 and 46). Our data suggest that a comparison of results for different carriers needs to take into account the differences in the frequency-domain representation of grating carriers and noise carriers and in particular the pattern of additional components induced by contrast modulation. We have shown that components of the carrier that have a lower spatial frequency than the envelope spatial frequency introduce components in the transform of the modulated carrier that are equivalent to adding motion in the envelope direction. These low-spatial-frequency components act against perceived reversals in the apparent direction of motion induced by increasing temporal frequency in situations in which high-spatial-frequency components (signaling motion in the same direction as that of the envelope) are attenuated or fall outside the window of visibility. Not only does this effect of low-spatial-frequency components remove any reversal, but in many cases it facilitates the perception of forward motion in an otherwise chaotic stimulus. Empirically, similar results are found for direction discrimination at high temporal frequencies for grating carriers and noise carriers when in each case a lower bound is placed on carrier spatial frequency content to exclude spatial frequencies lower than the envelope spatial frequency.

The window-of-visibility theory of stimulus detection and discrimination[37] can explain the majority of the data at high temporal frequencies, in particular the reversal seen in several of the conditions. This theoretical construct has been shown to be relevant in many situations, including other aspects of motion detection, most particularly the ability to discriminate sampled motion from smooth motion.[30,34,37] We believe that it is important to note at this stage that any model of motion detection in the visual system should explicitly implement some form of the window-of-visibility theory within its structure in

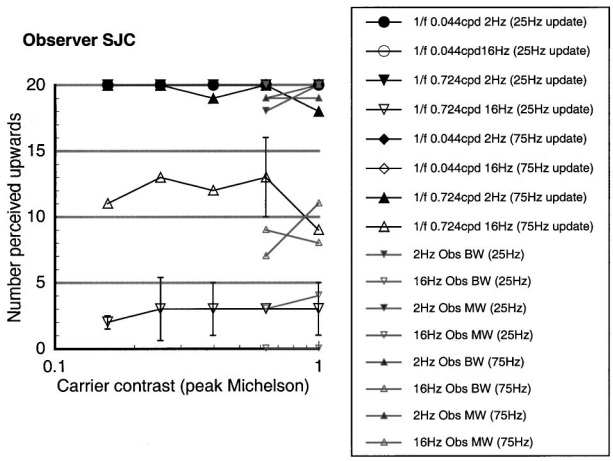

Fig. 15. Effect of carrier update rate on envelope direction discrimination for a 1/*f* noise carrier as a function of Michelson contrast. The perceived direction of envelope motion is plotted against the carrier contrast for low (2 Hz) and high (16 Hz) temporal envelope drift rates. The dynamic carrier is updated at 25 Hz (Fig. 3) and at 75 Hz as indicated. The main observer is SJC with supplementary observers BW and MW. Other details as in Fig. 3.

order to provide a close quantitative description of human performance in motion tasks.

As a final comment on the current paper, it is the case that if a noise carrier is updated at the same rate as a moving envelope with a new noise carrier on each frame, then the stimulus will be drift balanced whatever the spatial characteristics of the carrier.[6] However, preliminary data and data collected in response to an important question raised within the review process[63] has shown that the principal carrier dependence of all data presented here remains in a microbalanced stimulus. This is shown in Fig. 15.

Figure 15 plots the ability to perceive direction in a drifting (2-Hz and 16-Hz) envelope modulating a dynamic 1/*f* carrier for three observers as a function of contrast. The figure illustrates that there is no difference in the amount of perceived forward motion of the envelope when the carrier is updated either at 25 Hz or at 75 Hz, the latter being the truly microbalanced stimulus. There is a moderate reduction in the perceived reversal when the carrier update rate is increased. The interpretation of these microbalanced data in terms of the window of visibility is invalid if the mathematical description holds[6] within the neural image and holds for the analysis of the signal within the system. We are currently considering possible explanations for these data, and we intend to explore the significance of manipulation of the temporal spectrum of the stimulus.

ACKNOWLEDGMENTS

Simon J. Cropper was supported by an Australian Research Council QE2 Fellowship and Large Grant, and Alan Johnston is supported by a project grant from the Biotechnology and Biological Sciences Research Council/Engineering and Physical Sciences Research Council Mathematical Modelling Initiative. The authors thank John Wattam-Bell and Evan Thomas for helpful discussion, our reviewers for pertinent and largely helpful comments, and, in particular, Charlie Chubb for prompting extensive debate on the issue of drift-balanced stimuli. S. J. Cropper thanks Patti Smith for inspiration and for the subtitle. The basis of this work was initially presented at the Association for Research in Vision and Ophthalmology annual conference in Ft. Lauderdale, Fla., May 9–14, 1999.

REFERENCES

1. G. B. Henning, B. G. Hertz, and D. E. Broadbent, "Some experiments bearing on the hypothesis that the visual system analyses spatial patterns in independent bands of spatial frequency," Vision Res. **15**, 887–897 (1975).
2. S. J. Cropper, D. R. Badcock, and A. Hayes, "On the role of second-order signals in the perceived direction of motion of type II plaid patterns," Vision Res. **34**, 2609–2612 (1994).
3. A. T. Smith and T. Ledgeway, "Second-order motion: the carrier is crucial," Perception **24**, 28a (1995).
4. A. T. Smith and T. Ledgeway, "Separate detection of moving luminance and contrast modulations: fact or artefact?" Vision Res. **37**, 45–54 (1997).
5. S. J. Cropper and D. R. Badcock, "Perceived direction of motion: It takes all orientations," Perception **24**, 106a (1995).
6. C. P. Benton and A. Johnston, "First-order motion from contrast modulated noise?" Vision Res. **37**, 3073–3078 (1997).
7. D. R. Badcock and A. M. Derrington, "Detecting the displacement of periodic patterns," Vision Res. **25**, 1253–1258 (1985).
8. D. R. Badcock and A. M. Derrington, "Detecting the displacements of spatial beats: a monocular capability," Vision Res. **27**, 793–797 (1987).
9. D. R. Badcock and A. M. Derrington, "Detecting the displacements of spatial beats: no role for distortion products," Vision Res. **29**, 731–739 (1989).
10. A. M. Derrington and D. R. Badcock, "Separate detectors for simple and complex grating patterns?" Vision Res. **25**, 1869–1878 (1985).
11. A. M. Derrington and D. R. Badcock, "Detection of spatial beats: non-linearity or contrast increment detection?" Vision Res. **26**, 343–348 (1986).
12. A. M. Derrington, D. R. Badcock, and G. B. Henning, "Discriminating the direction of second-order motion at short stimulus durations," Vision Res. **33**, 1785–1794 (1993).
13. C. Chubb and G. Sperling, "Drift-balanced random stimuli: a general basis for studying non-Fourier motion perception," J. Opt. Soc. Am. A **5**, 1986–2006 (1988).
14. Z.-L. Lu and G. Sperling, "The functional architecture of human visual motion perception," Vision Res. **35**, 2697–2722 (1995).
15. P. Werkhoven, G. Sperling, and C. Chubb, "The dimensionality of texture-defined motion: a single channel theory," Vision Res. **33**, 463–485 (1993).
16. T. Ledgeway and A. T. Smith, "The duration of the motion aftereffect following adaptation to first-order and second-order motion," Perception **23**, 1211–1219 (1994).
17. T. Ledgeway, "Adaptation to second-order motion results in a motion aftereffect for directionally ambiguous test stimuli.," Vision Res. **34**, 2879–2889 (1994).
18. T. Ledgeway and A. T. Smith, "Evidence for separate motion-detecting mechanisms for first and second-order motion in human vision," Vision Res. **34**, 2727–2740 (1994).
19. T. Ledgeway and A. T. Smith, "The perceived speed of second-order motion and its dependence on stimulus contrast," Vision Res. **35**, 1421–1434 (1995).
20. T. Ledgeway and A. T. Smith, "Changes in perceived speed following adaptation to first-order and second-order motion," Vision Res. **37**, 215–225 (1997).
21. G. J. Burton, "Evidence for non-linear response processes in the human visual system from measurements on the thresholds of spatial beat frequencies," Vision Res. **13**, 1211–1225 (1973).

22. D. I. A. MacLeod, D. R. Williams, and W. Makous, "A visual non-linearity fed by single cones," Vision Res. **32**, 347–363 (1992).
23. S. J. Cropper and S. T. Hammett, "Adaptation to motion of a second order pattern: The motion aftereffect is not a general result," Vision Res. **37**, 2247–2259 (1997).
24. S. J. Cropper, "The detection of luminance and chromatic contrast modulation by the visual system," J. Opt. Soc. Am. A **15**, 1969–1986 (1998).
25. A. Johnston and C. W. G. Clifford, "Perceived motion of contrast-modulated gratings: predictions of the multichannel gradient model and the role of full-wave rectification," Vision Res. **35**, 1771–1784 (1995).
26. A. Johnston, C. P. Benton, and M. J. Morgan, "Concurrent measurement of perceived speed and speed discrimination threshold using the method of single stimuli," Vision Res. **39**, 3849–3855 (1999).
27. H. R. Wilson and J. Kim, "Perceived motion in the vector-sum direction," Vision Res. **34**, 1835–1842 (1994).
28. H. R. Wilson, V. P. Ferrera, and C. Yo, "A psychophysically motivated model for two-dimensional motion perception," Visual Neurosci. **9**, 79–97 (1992).
29. A. M. Derrington, J. Krauskopf, and P. Lennie, "Chromatic mechanisms in lateral geniculate nucleus of macaque," J. Physiol. (London) **357**, 241–265 (1984).
30. S. J. Cropper and D. R. Badcock, "Discriminating smooth from sampled motion: chromatic and luminance stimuli," J. Opt. Soc. Am. A **11**, 515–530 (1994).
31. C. F. I. Stromeyer, A. Chaparro, A. Tolias, and R. E. Kronauer, "Equiluminant settings change markedly with temporal frequency," Invest. Ophthalmol. Visual Sci. Suppl. **36**, 962 (1995).
32. W. H. Press, S. A. Teukolsky, W. T. Vetterling, and B. P. Flannery, *Numerical Recipes in C: The Art of Scientific Computing* (Cambridge U. Press, Cambridge, UK, 1992).
33. S. J. Cropper and A. M. Derrington, "Detection and motion detection in chromatic and luminance beats," J. Opt. Soc. Am. A **13**, 401–407 (1996).
34. S. J. Cropper and A. Johnston, "The detection of the motion of chromatic and luminance contrast modulation by the visual system," manuscript available from the authors.
35. D. J. Fleet and K. Langley, "Computational analysis of non-Fourier motion," Vision Res. **34**, 3057–3079 (1994).
36. R. N. Bracewell, *The Fourier Transform and Its Applications* (McGraw-Hill, New York, 1978).
37. A. B. Watson, A. Ahumada, and J. E. Farrell, "Window of visibility: a psychophysical theory of fidelity in time-sampled visual displays," J. Opt. Soc. Am. A **3**, 300–307 (1986).
38. A. M. Derrington and G. B. Henning, "Errors in direction-of-motion discrimination with complex stimuli," Vision Res. **27**, 61–75 (1987).
39. A. M. Derrington and G. B. Henning, "Further observations on errors in direction-of-motion discrimination," Invest. Ophthalmol. Visual Sci. Suppl. **28**, 298 (1987).
40. J. M. Findlay, "Estimates on probability functions: a more virulent PEST," Percept. Psychophys. **23**, 181–185 (1978).
41. N. Brady and D. J. Field, "What's constant in contrast constancy? The effects of scaling on the perceived contrast of bandpass patterns," Vision Res. **35**, 739–756 (1995).
42. I. Kovacs and A. Feher, "Non-Fourier information in bandpass noise patterns," Vision Res. **37**, 1167–1175 (1997).
43. J. G. Robson, "Spatial and temporal contrast sensitivity functions of the visual system," J. Opt. Soc. Am. **56**, 1141–1142 (1966).
44. A. T. Smith and T. Ledgeway, "Sensitivity to second-order motion as a function of temporal frequency and eccentricity," Vision Res. **38**, 403–410 (1998).
45. O. I. Ukkonen and A. M. Derrington, "Motion of contrast-modulated grating is analysed by different mechanisms at low and at high contrasts," Vision Res. **40**, 3359–3371 (2000).
46. I. E. Holliday and S. J. Anderson, "Different processes underlie the detection of second-order motion at low and high temporal frequencies," Proc. R. Soc. London Ser. B **257**, 165–173 (1994).
47. C. Chubb and G. Sperling, "Drift-balanced random stimuli: A general basis for studying non-Fourier motion perception," J. Opt. Soc. Am. A **5**, 1986–2006 (1988).
48. S. J. Cropper and A. M. Derrington, "Motion of chromatic stimuli: first-order or second-order?" Vision Res. **34**, 49–58 (1994).
49. S. J. Cropper, K. T. Mullen, and D. R. Badcock, "Motion coherence across cardinal axes," Vision Res. **36**, 2475–2488 (1996).
50. K. T. Mullen, "The contrast sensitivity of human color vision to red/green and blue/yellow chromatic gratings," J. Physiol. (London) **359**, 381–400 (1985).
51. R. T. Eskew, C. F. Stromeyer III, and R. E. Kronauer, "Temporal properties of the red–green chromatic mechanism," Vision Res. **34**, 3127–3137 (1994).
52. C. Yo and H. R. Wilson, "Perceived direction of moving two-dimensional patterns depends on duration, contrast and eccentricity," Vision Res. **32**, 135–147 (1992).
53. A. Johnston, C. P. Benton, and P. W. McOwan, "Induced motion at texture-defined motion boundaries," Proc. R. Soc. London Ser. B **266**, 2441–2450 (1999).
54. C. Blakemore and F. W. Campbell, "On the existence of neurones in the human visual system sensitive to the orientation and size of retinal images," J. Physiol. (London) **203**, 237–260 (1969).
55. P. Cavanagh, "Attention-based motion perception," Science **257**, 1563–1565 (1992).
56. B. Hassenstein and W. Reichardt, "Systemtheoretische Analyse der zeitreihenfolgen und vorzeichenauswertung bei der Bewegungspwezeption des Rüssekafers *Chlorophanus*," Z. Naturforsch. **11b**, 513–524 (1956).
57. W. Reichardt, "Autocorrelation, a principle for the evaluation of sensory information by the central nervous system," in *Sensory Communication*, W. A. Rosenblith, ed. (Wiley, New York, 1961).
58. D. Marr and S. Ullman, "Directional selectivity and its use in early visual processing," Proc. R. Soc. London Ser. B **211**, 151–180 (1981).
59. A. Johnston, P. W. McOwan, and H. Buxton, "A computational model for the analysis of some first-order and second-order motion patterns by simple and complex cells," Proc. R. Soc. London Ser. B **250**, 297–306 (1992).
60. S. J. Cropper, "Human motion detection: different patterns, different detectors?" Ph.D. dissertation (University of Newcastle upon Tyne, Newcastle upon Tyne, UK, 1992).
61. A. T. Smith, R. F. Hess, and C. L. Baker, Jr., "Direction identification thresholds for second-order motion in central and peripheral vision," J. Opt. Soc. Am. A **11**, 506–514 (1994).
62. A. M. Derrington and M. J. Cox, "Temporal resolution of dichoptic and second-order motion mechanisms," Vision Res. **38**, 3531–3539 (1998).
63. C. F. Chubb, Department of Cognitive Sciences, University of California, Irvine, California 92697 (personal communication, May 2001).